Available online at www.sciencedirect.com
SCIENCE DIRECT®
Polymer 44 (2003) 7757–7764
polymer
www.elsevier.com/locate/polymer

Physical interactions at carbon nanotube-polymer interface

M. Wong[a], M. Paramsothy[b], X.J. Xu[d], Y. Ren[c], S. Li[b], K. Liao[c,*]

[a]*Department of Mechanical Engineering, Polymer Technology Center, Texas A and M University, College Station TX 77843-3123, USA*
[b]*School of Materials Engineering, Nanyang Technological University, Singapore 639798, Singapore*
[c]*School of Mechanical and Production Engineering, Nanyang Technological University, 50 Nanyang Avenue, Singapore 639798, Singapore*
[d]*Nano/Micro Mechanics Laboratory, Faculty of Engineering, National University of Singapore, Singapore 117576, Singapore*

Received 19 April 2003; received in revised form 9 July 2003; accepted 8 October 2003

Abstract

Mechanical properties of carbon nanotube (CNT) reinforced polystyrene rod and CNT reinforced epoxy thin film were studied and the CNT-polymer interface in these composites was examined. Transmission and scanning electron microscopy examinations of CNT/polystyrene (PS) and CNT/epoxy composite showed that these polymers adhered well to CNT at the nanometer scale. Molecular mechanics simulations and elasticity calculations were used to quantify some of the important interfacial characteristics that critically control the performance of a composite material. In the absence of chemical bonding between CNT and the matrix, it is found that the non-bond interactions, consist of electrostatic and van der Waals forces, result in CNT-polymer interfacial shear stress (at 0 K) of about 138 and 186 MPa, respectively, for CNT/epoxy and CNT/PS. The high interfacial shear stress calculated, about an order of magnitude higher than micro fiber reinforced composites, is believed attributed to intimate contact between the two solid phases at the molecular scale. Simulations and calculations also showed that local non-uniformity of CNT and mismatch of the coefficients of thermal expansions between CNT and polymer matrix also promote the stress transfer ability between the two.

Keywords: Carbon nanotube; Polymer composites; Interface

1. Introduction

Carbon nanotubes (CNTs), discovered in 1991 [1], are seamlessly rolled sheets of hexagonal array of carbon atoms with diameter ranging from a few Angstroms to several tens of nanometers across. These nanometer-sized tubes exist in two forms, single-walled carbon nanotube (SWNT) in which the tube is formed from only a single layer of carbon atoms, and multi-walled carbon nanotubes (MWNT), in which the tube consists of several layers of coaxial carbon tubes [1,2]. The high strength and elastic modulus of these tubes render them ideal candidate as ultra-strong reinforcement for composites [3–6]. It is well established, from decades of research on micro fiber reinforced composites, that fiber-matrix interfacial shear stress is a critical parameter controlling the efficiency of stress transfer and hence some of the important mechanical properties of the composite such as elastic modulus, tensile strength, fracture toughness, as well as their long-term behavior. Current interests in using CNTs and anticipated potential applications for CNT reinforced polymer composites demand a better understanding of the CNT-matrix interfacial characteristics. However, the physics of interactions between CNT and its surrounding matrix material in such nano-composites has yet to be elucidated, and methods for determining the parameters controlling interfacial characteristics such as interfacial shear stress, is still challenging.

Previous studies on CNT-polymer composite systems suggested that chemical bonding between CNT and the polymer matrix may or may not exist, and adhesion between CNT and certain polymer systems are strong, although there are also contrasting views. Upon close examination of the fracture surface of a MWNT/polyhydroxyaminoether composite, Bower et al. observed contact and adherence of the polymer to most of the nanotubes, and in some cases the entire surface of the nanotube was covered with a layer of polymer [7]. Chang et al. also observed CNT was well coated by polypyrroles in a CNT/polypyrroles composite produced by in situ polymerization. Raman scattering and

* Corresponding author. Tel.: +65-67905835; fax: +65-67911859.
E-mail address: askliao@ntu.edu.sg (K. Liao).

0032-3861/$ - see front matter © 2003 Elsevier Ltd. All rights reserved.
doi:10.1016/j.polymer.2003.10.011

X-ray diffraction data suggested there is no chemical reaction between CNT and the polymer [8]. In a study by Jia et al. [9], CNT was used as a reinforcement for poly(methyl methacrylate) (PMMA), also by an in situ polymerization process. Chemical bonding between CNT and PMMA was confirmed using infrared transmission spectra. It was proposed that π-bond of CNT was opened due to the initiation of 2,2′-azobisisobutyronitrile (AIBN) and linked to each other (PMMA and AIBN), thus producing a stronger CNT-PMMA interface.

From mechanics point of view, available literatures to date also offered evidence of strong CNT–polymer interactions. Lourie and Wagner first showed CNT fragmentation in epoxy matrix, implying that force was transmitted to the CNT from the surrounding matrix [10,11]. From fragmentation experiments, these authors estimated that the CNT-matrix stress transfer ability is at least one order of magnitude larger than that measured in conventional micro fiber-based composites. Compared to CNT-polymer interface, they attribute the lower interfacial strength of conventional micro fiber-polymer interface to larger defects that facilitate interfacial crack propagation [10]. Furthermore, Qian et al. [12] showed that tensile load can be transferred effectively from the polystyrene (PS) matrix to the CNT, resulting in high elastic modulus increase (42%) using just 1 wt% (percent by weight) CNT. Similar results were also shown by Xu et al. [13], using CNT/epoxy thin film composite system. Using an expanded form of Kelly–Tyson approach, Wagner [14] showed that high interfacial shear strength between CNT and polymers is possible, in agreement with results from molecular mechanics simulation of CNT pullout [15,16]. More recently, Cooper et al. [17] showed that interfacial shear strength between MWNT and epoxy ranged from 35–376 MPa, from pullout experiments using atomic force microscope. Despite these positive evidences of strong CNT–polymer interactions, that CNT-polymer interface only offers poor stress transfer was also reported. Based on evidence of micro Raman spectroscopy, Schadler et al. [18,19] showed that load transfer between CNT-epoxy was poor.

Although these studies have provided some insights into the nature of CNT–polymer interactions at the interface, the physics of CNT–polymer interactions still await further elucidation, both qualitatively and quantitatively. In this paper, we present results of a study on the interfacial morphology of CNT/PS and CNT/epoxy composites. Molecular mechanics simulations of CNT pullout from the polymer matrices and elasticity calculations of thermal residual stress between the nano reinforcement and the polymer matrix are also carried out for quantitative analysis.

2. Experimental

Two different types of CNT/polymer composite samples were fabricated and their mechanical properties studied, detailed as follows.

2.1. CNT/polystyrene composite

MWNT were synthesized by pyrolysis of hydrocarbon. Methane (CH_4) gas was passed over a hot powder catalyst of Ni particles supported by MgO, maintained at 700 °C. The raw carbon powders obtained after carbon deposition were purified by stirring in warm dilute nitric acid for several hours to dissolve the catalyst particles. After acid dissolution, the carbon powders were washed with distilled water and dried at an elevated temperature for a few hours in an argon atmosphere. The results were random coiled MWNTs with diameter ranging from 20 to 60 nm and length ranging from 1 μm to several tens of microns (Fig. 1), with 96 wt% purity. Little (less than 4 wt%) non-CNT materials such as catalyst particles and amorphous carbon were observed from transmission electron microscope (TEM) images and thermogravimetric analysis (TGA).

To fabricate CNT/PS composite, 6 g of PS was dissolved in 40 g of toluene, and the mixture was placed on a hot plate with stirrer in the beaker. Temperature and stir speed were controlled so that the PS dissolved completely in about 30 min to form a clear solution. Appropriate amount of CNT was weighed according to the required percentage and was added to the solution. The mixture was then stirred for 1 h to form a homogeneous suspension. The suspension was sonicated for 1 h and was then cast into an aluminum mould in the form of a film. The mould with the suspension was baked in an oven at 100 °C for 3 h. The baked sample was then removed from the mould and cut into rectangular pieces approximately 3 mm by 5 mm. The cut-up samples were then extruded in a mini extruder at 180 °C under an

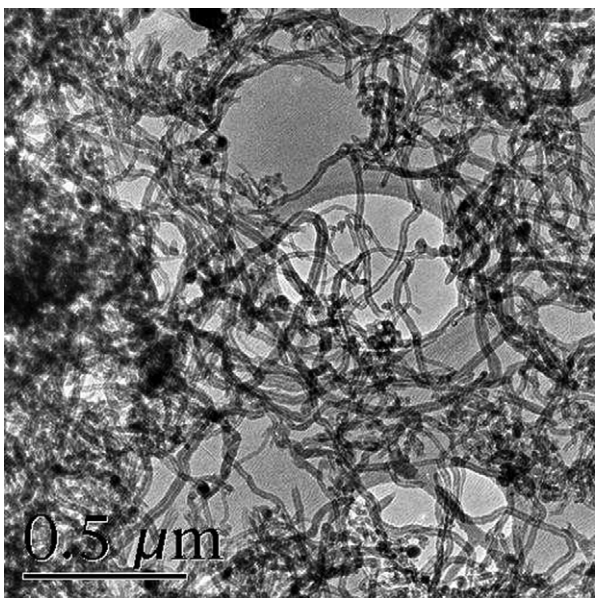

Fig. 1. TEM image of MWNT synthesized by pyrolysis of CH_4. Bends and kinks as well as diameter variations can be seen along the CNTs.

extrusion load of 30N. The reservoir of CNT/polymer melt was extruded through a die of 1 mm (diameter) by 10 mm (depth) with a pressure of 7.4×10^4 Pa. Composite rods with approximately 0.1, 0.5, 1.0, and 2.0 wt% of CNT were obtained.

Tensile tests were performed on these rod samples in a tensile tester (Instron™). These 1 mm-diameter composite rods were loaded to failure at a cross-head speed of 1 mm/min, and the tensile strain was recorded by a video extensometer. At least 8 samples were tested for each composition. Tensile failure surfaces of the CNT/PS composite rod were examined under a field emission scanning electronic microscope (FESEM) and TEM. To prepare for TEM imaging, composite samples were embedded in an epoxy (Struer Epofix Kit) and were cut into thin slices at room temperature by a microtom (Leica Ultracut UCT) with a cutting speed of 2 mm/s. The thickness of the slices was controlled by the feeding step, set at 70 nm.

2.2. CNT/epoxy thin film

Epoxy thin films containing 0.1 wt% MWNT synthesized from pyrolysis of hydrocarbon, as described in the previous paragraphs, were prepared. Detailed procedures for fabricating MWNT/epoxy thin film have been described elsewhere [13]. Briefly, a mixture of MWNT and EPON SU-8, a commercially available photoresist epoxy resin, was spin coated onto a clean, standard 4-inch silicon wafer. The silicon substrate was etched from the backside of thin film-substrate system by Deep Reactive Ion Etching (DRIE) after the epoxy was cured, leaving a circular thin film on the rigid substrate, which has a hole of 8 mm in diameter. The thickness of the composite and pure epoxy films was 5.8 and 12.5 μm, respectively, estimated from SEM images.

Thin film samples were tested using a shaft-loaded blister method [20]. Load was applied onto the center of the thin film at a cross-head speed of 0.1 mm/min via an aluminum shaft with a 3.2 mm-diameter stainless steel ball fixed at one end as the loading point, using a micro force tester (Instron™). The film was loaded until puncture at the center. Fracture surface of CNT/epoxy samples was studied under SEM and samples were microtomed for TEM examinations.

3. Results and discussion

3.1. Morphology of CNT-polymer Interface

Results of tensile tests for CNT/PS rod samples are summarized in Table 1, and a typical stress–strain curve is shown in Fig. 2. In general all of the samples showed a decrease in both tensile stiffness and strength, except those with 0.1 wt% CNT, where a moderate increase in tensile

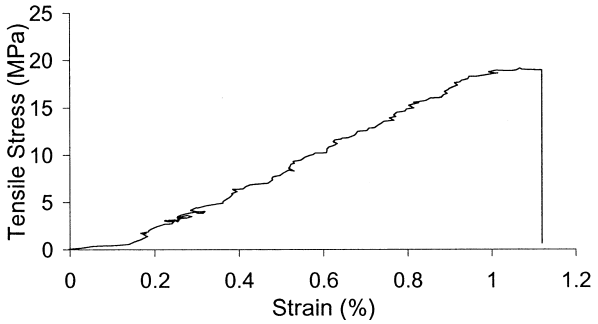

Fig. 2. A typical stress–strain curve from tensile test of a CNT/PS composite rod.

strength (about 10%), and a slight increase in tensile stiffness (about 2%) and failure strain (about 3%) are seen. Although the extrusion process is believed to align CNTs somewhat in the flow direction, from FESEM images, it is seen that CNTs still exist in the form of agglomerates, ranging approximately from 5 to 20 μm in diameter (Fig. 3(a)). The reinforcing effect of the CNT agglomerate, if any, was offset by the fact that they were also acting as flaws or stress concentrators in the composite. The fact that failure strain and tensile strength decrease with an increase in CNT content suggest that CNT were not well dispersed in the matrix.

In Fig. 3(b), radiating hackles on the PS fracture surface originated from the CNT agglomerate and voids inside CNT agglomerate are clearly seen. The pattern of fracture shown in Fig. 3(b) is comparable to the mirror-mist-hackle pattern of brittle fracture: the ‘mirror’ is a region containing a flaw over which the flaw propagates slowly; the ‘mist’ is a transition region between the mirror region and the fast crack propagation region with the ‘hackle’ morphology. In the present case the ‘fracture mirror’ is analogous to the CNT agglomerate itself and the mist is the boundary between the CNT agglomerate and the polymer matrix. A bundle of CNTs being pulled out from the agglomerate is shown in Fig. 4, where the individual CNT is more or less aligned with the loading direction, implying that these CNTs were in fact exerting some degrees of reinforcing effect for the matrix material.

Close examination of individual CNT in the agglomerate revealed that they are all coated by PS, suggesting good wetting of CNT by PS and that surface energies favor CNT-PS contact. Failure around the CNT agglomerate occurred within the PS matrix but not between CNT and its PS coating, suggesting strong CNT-PS adhesion. Although atomic defects of CNT that resulted in local tube non-uniformity were found, extensive examinations of the CNT/PS interface by TEM, indicate that these CNTs are in intimate contact with the PS matrix, suggesting excellent adherence between CNT and PS. In Fig. 5(a), cross sectional view of a CNT (located in the middle of the image) embedded in the PS matrix is shown. The circumference of the CNT is seen in close contact with the matrix, with no

Table 1
Results of tensile test of CNT/PS composite rods

CNT content (wt%)	Sample tested	Failure strain[a] (%)	Tensile strength[a] (MPa)	Elastic modulus[a] (GPa)
2.0	8	1.20	18.8	2.18
1.0	8	1.20	21.6	2.35
0.5	8	1.27	17.9	2.01
0.1	8	1.35	24.4	2.47
0.0	10	1.31	22.1	2.42

[a] Average value.

obvious gaps observed at nanometer resolution. The darker regions in Fig. 5(a) are other CNTs embedded in the matrix. Again, they are seen tightly bound to the matrix. A longitudinal section of a CNT in PS is shown in Fig. 5(b), where a change in tube diameter due to defect is obvious. This kind of mechanical interlocking is believed to contribute to the CNT-polymer adhesion. More will be said on this later.

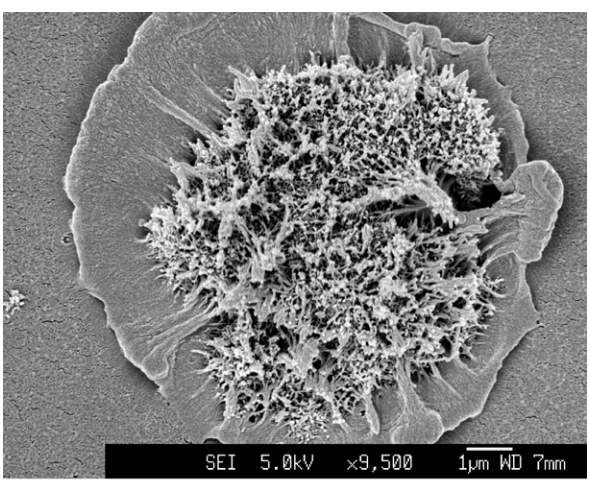

(a)

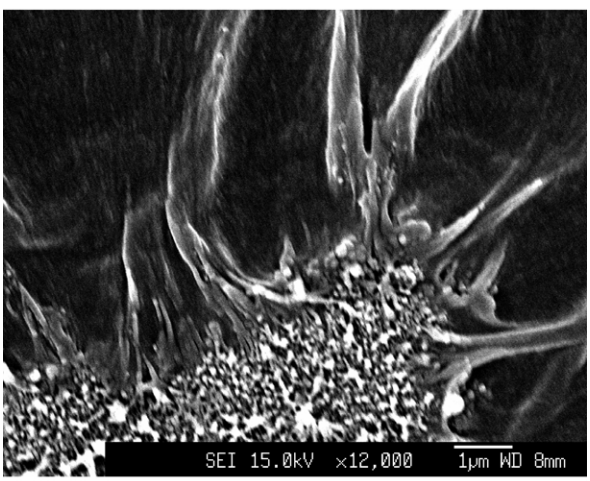

(b)

Fig. 3. FESEM images of fracture surface of CNT-PS composite: (a) a CNT agglomerate being pulled half way out from the PS matrix, (b) details of the hackle formed on the PS matrix.

Results of shaft-loaded blister test on epoxy and CNT/epoxy thin films showed that 0.1 wt% of CNT can increase the elastics modulus of the epoxy thin film by as much as 20%, suggesting that CNTs were aligned in the radial direction upon spin coating [13]. On the other hand, however, CTN/epoxy thin film has lower failure strain than neat epoxy thin film. Scanning electron microscopy (SEM) observations of the fracture mode showed that cracks originated at the contact region between the shaft ball and the thin film, and propagated in the radial direction to the edge of film-silicon boundary. MWNTs were found confined parallel to the plane of the thin film, and most MWNTs were seen running longitudinally along radial directions of the circular thin film, that is, they were oriented perpendicular to the crack direction, a consequence of CNT realignment under the action of centrifugal force during spin coating.

MWNT fracture and pullout near the matrix crack are shown in Fig. 6. Similar to the previous case of CNT/PS rod, most pullout ends observed were covered by epoxy, indicating failure of the matrix but not the CNT-epoxy interface, suggesting a stronger interfacial adhesion between MWNT and the matrix. However, MWNT agglomerates also existed at places, where 'clean' MWNTs were found directly separated from the matrix, a

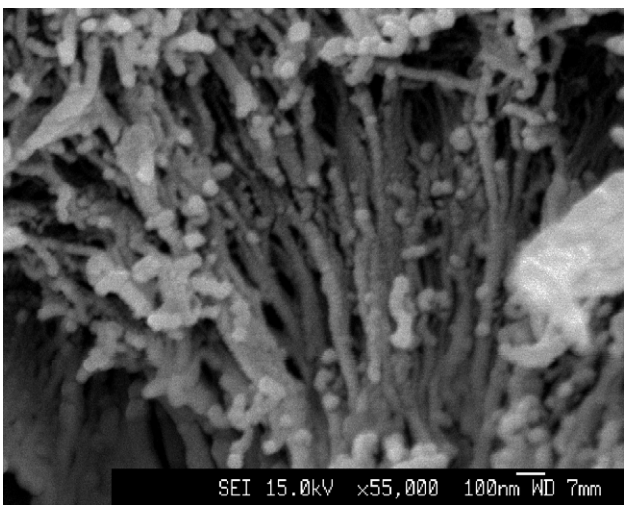

Fig. 4. FESEM image of CNT bundles, note that most tubes are coated with PS. Scale bar is 100 nm.

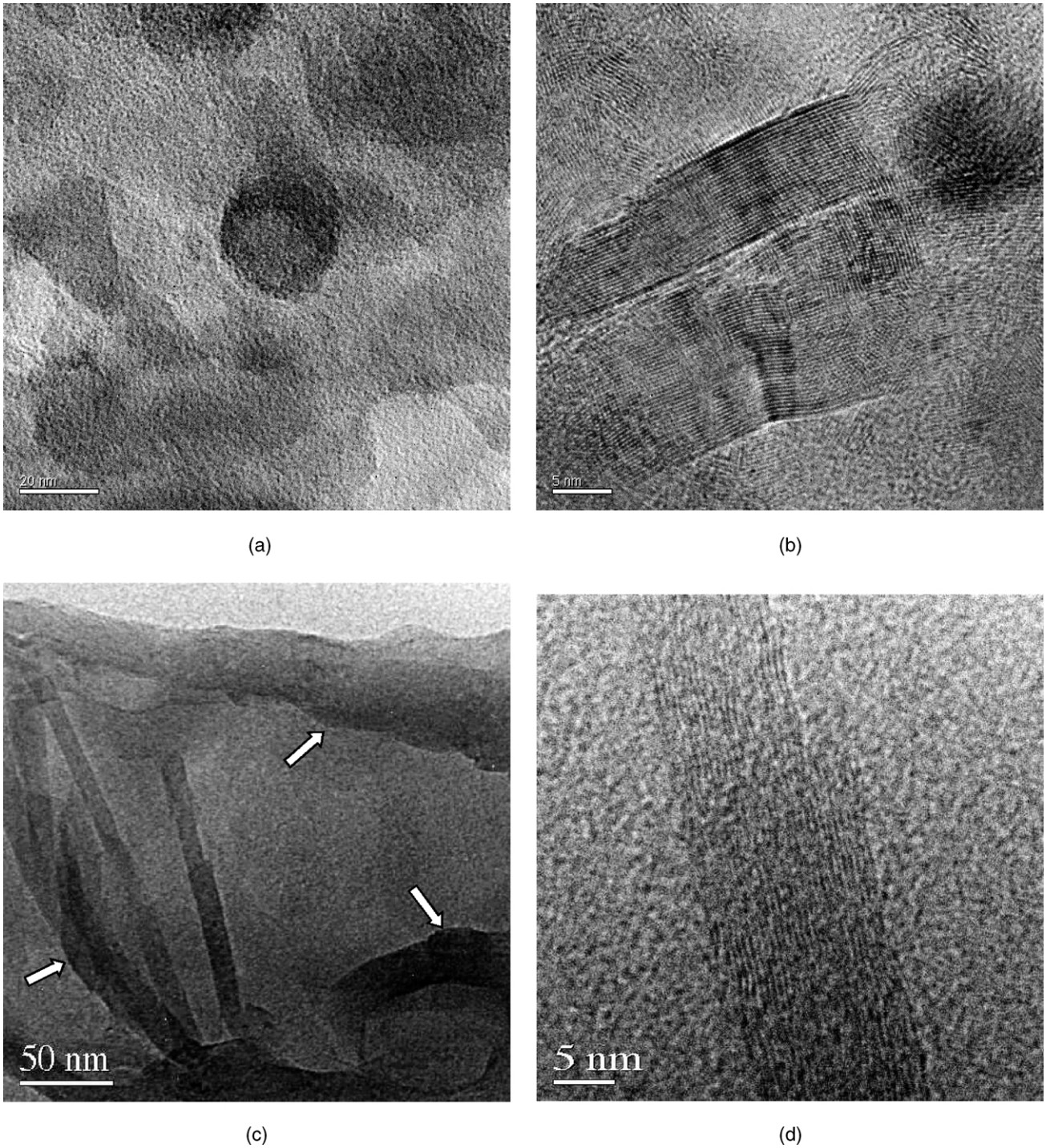

Fig. 5. TEM images of CNTs embedded in PS or epoxy. (a) Dark circular region in the middle is the cross section of a CNT embedded in PS matrix. Other dark regions are other randomly oriented CNTs (scale bar is 20 nm). (b) Details of CNT-PS interface, note the kink and change in diameter of the CNT, which is believed to promote mechanical interlocking. (c) TEM images of CNT/epoxy interface: non-uniform CNT diameter and bends (indicated by arrows) can be seen. (d) A longitudinal section of CNT (located in the middle) is seen covered by epoxy molecules, thus the CNT-polymer interface is not clearly distinguishable. In most TEM images that we have examined, no physical gaps between CNT and the polymer matrix are found, indicating good adhesion between the two.

result of poor local dispersion of MWNT, and was probably the cause of failure initiation.

TEM images of CNT embedded in epoxy are shown in Fig. 5(c) and (d). Covered by epoxy molecules, it is seen from these images that the lattice of the CNTs is blurred, and so are the boundaries between the nanotubes and the epoxy matrix. Similar to the case of CNT/PS, extensive examination under TEM did not reveal clear physical gaps

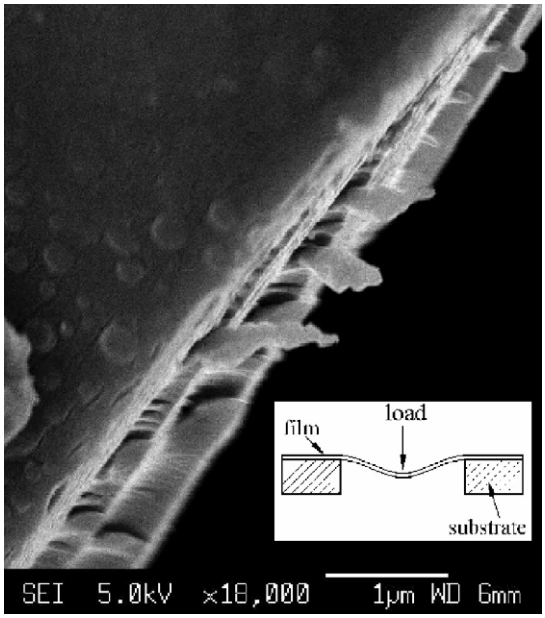

Fig. 6. Fracture surface of CNT/epoxy thin film, oriented in radial direction. CNT bundles are seen coated with epoxy. Inset: schematic of the test setup.

between CNT and epoxy molecules. It was known that microtoming introduce shear force to the material and may result in CNT pullout from the matrix [21]. However, no obvious CNT pullout from the epoxy was observed in the CNT/epoxy slices after microtoming, and most of the CNTs remained in the epoxy, suggesting good adherence of the polymer to CNT. From these morphology studies, it can be concluded that PS and epoxy adhere well to individual CNT. In what follows, we further elaborate several contributing mechanisms for CNT-polymer adhesion in more detail.

3.2. Mechanical interlocking

Local non-uniformity along a CNT, including varying diameter and bends/kinks at places as a result of non-hexagonal defects, contribute to CNT-polymer adhesion by mechanical interlocking. This is shown in Figs. 1 and 5(b). In the case of CNT pullout, for instance, extra mechanical work has to be provided for CNT and the polymer to deform at 'rough contacts' in order for them to slip pass each other, compared to CNT-polymer contact along a smooth CNT surfaces.

To illustrate the idea, a molecule model of a CNT with diameter variation embedded in an array of linear polyethylene is constructed and the CNT was pulled through the polymer 'brush' from the end with smaller diameter. The diameters of the larger and smaller ends of the CNT are 20.1 and 13.3 Å, respectively, and its length is about 31 Å. The CNT was drawing through the polymer brush in a stepwise manner and energy minimization was performed at each step using MM +, an empirical force potential. This is because (1) MM + is very close to the second generation Brenner potential for carbon [22], and (2) it is primarily used for organic materials, thus is ideal for studying CNT–polymer interactions [23].

As the CNT and the polymer are being displaced relative to each other against the interlock (represented by the changing CNT diameter), extra energy is needed to deform the polymer. This is seen in Fig. 7, where a jump in potential energy of the system is seen when the portion of CNT with larger diameter is draw closer into the polymer and causes deformation of the polymer. Close contact of CNT and polymer and largely non-uniformity in CNTs suggest that mechanical interlocking could be an important contributor for CNT-polymer adhesion.

3.3. Thermal effects

Mismatch in the coefficients of thermal expansion (CTE) between CNT and polymer results in thermal residual radial stress and deformation along the tube when the polymer is cooled from its melt. Compressive radial stress results in closer CNT-polymer contact which could enhance CNT–polymer non-bond interactions; and local CNT deformation which promotes mechanical interlocking.

To calculate radial stress using the concentric cylinder model based on elasticity theory [24], the elastic modulus in the radial direction of CNT, E_r, need to be known. From Lu [25], the stiffness coefficient perpendicular to the basal plane, C_{33}, of a SWNT is 0.397 TPa. E_r is related to C_{ij} by:

$$E_r = C_{33} - [2C_{13}^2/(C_{11} + C_{12})] \quad (1)$$

From data of graphite crystal [26], the contribution from the second term of the previous equation is less than 1%, therefore E_r for SWNT is taken as 0.39 TPa in our

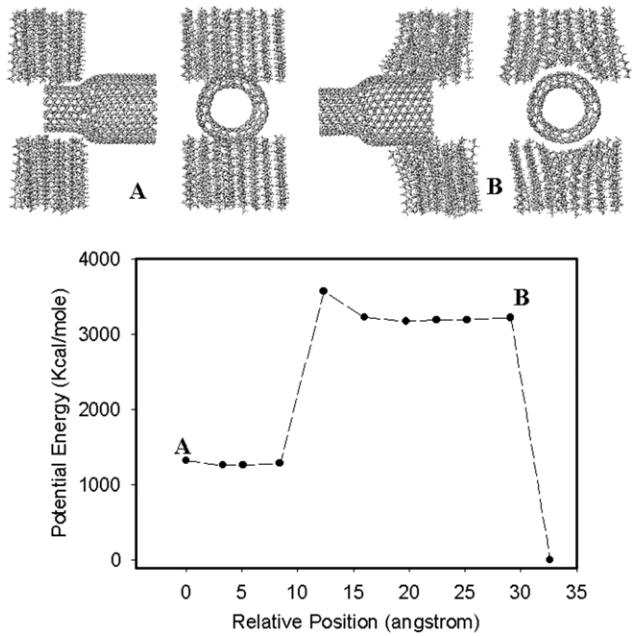

Fig. 7. A molecular model of a CNT embedded in two layers of short linear polyethylene array. Extra energy is needed to pull the CNT through the 'interlock'. **A** is point of entry and **B** is near-pullout position.

calculations. The longitudinal and transverse Young's modulus of SWNT were taken as 1 and 0.41 Tpa, respectively, and the Poisson's ratio of a SWNT is taken as 0.16 [25].

To the authors' knowledge, there is no measured CTE data currently available for CNT. Since CNT has a similar hexagonal arrangement of carbon atoms as the graphite crystal, the CTE of graphite crystal, such as α_c of 25×10^{-6}/K (15–800 °C) in *c*-axis and α_a of -1.5×10^{-6}/K (0–150 °C) in *a*-axis [26], were used as CTE of CNT in the calculation. The CTEs of PS and SU-8 are 28 and 52×10^{-6}/K, respectively [27]. From concentric cylinder model of elasticity, the radial stresses for SWNT/PS and SWNT/epoxy are estimated to be about −45 and −26 MPa /K. Hence thermal residual stress from CTE mismatch could be a significant factor contributing to CNT-polymer adhesion, in terms of promoting closer contacts and thus mechanical interlocking mechanisms. Moreover, closer contact also enhances non-bond interactions, discussed as follows.

3.4. Molecular simulations of CNT pullout

To date, devising experiments to determine CNT-polymer adhesion is still difficult, despite some recent progresses [17]. To quantify the adhesion between a CNT and its surrounding matrices, molecular model of SWNT/PS and SWNT/epoxy composites were constructed (Fig. 8), and CNT pullout from the matrices was simulated. Detailed simulation procedure has been described elsewhere [15]. In the absence of chemical bonding, the potential energy comes from non-bond interactions including electrostatic and van der Waal's force.

The energy difference between fully embedded CNT and the completely pullout configuration is taken as the work required for fiber pullout. The total work done, W, in pulling out the carbon nanotube from the polymer matrix can be related to the interfacial shear stress, τ_i, by the relation

$$W = \int_{x=0}^{x=L} 2\pi r(L-x)\tau_i \mathrm{d}x \tag{2}$$

or

$$W = \pi r \tau_i L^2$$

where r and L are the outer radius and length of the carbon nanotube, respectively, and x is the coordinate along the longitudinal tube axis. The shear stress between the CNT and the polymer, τ_i, estimated from the aforementioned correlation is about 186 MPa for SWNT/PS and 138 MPa for SWNT/epoxy, which is comparable to $\tau_i = 500$ MPa for the CNT/polyurethane system, estimated by Wagner et al. [10] from fragmentation experiments. The simulation results are also in agreement with results of a recently study by Cooper et al. [17], who showed that CNT/epoxy ranged from 35 to 376 MPa, from CNT pullout experiments using atomic force microscope. The results shown here is from 0 K, data showed that τ_i could be considerably higher at elevated temperatures [28].

What we have not considered in the molecular simulation are the influence of CNT geometry such as wall thickness (i.e. number of layers) and critical aspect ratio (ratio of critical stress transfer length to tube diameter) on interfacial shear stress distribution, both of which have been shown to affect stress transfer behavior based on continuum mechanics approach [14,29]. It should be point out that Eq. (2) for evaluating τ_i is based on an average shear stress assumption. To deduce shear stress distribution directly from molecular simulations could be challenging because: (1) one needs to use a tube (and matrix) model with much longer length, which is computationally very demanding; and (2) atomic displacements of the polymers in the vicinity of the nano reinforcement before and after pullout need to be handled one by one.

From mechanical testing of rod and film composite samples, the stiffness of PS (in one occasion) and epoxy is enhanced by CNT, indicating stress transfer capability from the polymer to CNT. However, the fact that significant enhancement in tensile strength was not seen in CNT/PS rod (in most cases) and lowered stress at puncture for CNT/epoxy film suggest that if not well dispersed, CNT aggregates may act as micron-sized flaws that are prone for crack initiation despite seemingly good local CNT-polymer adhesion at the nanometer scale.

Taken together, the following physical events all contribution to CNT–polymer interactions at the nanometer scale:

1. Under no chemical bonding between CNT-polymer, the origins of CNT–polymer interactions are electrostatic and van der Waals forces.
2. Local non-uniformity of a CNT embedded in polymer

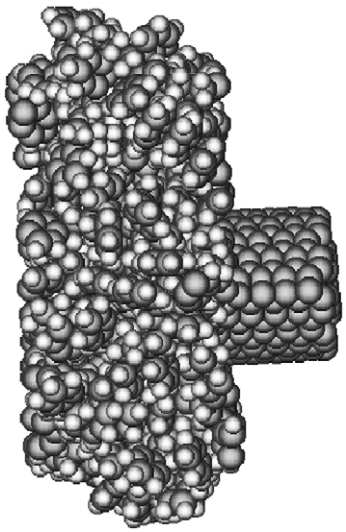

Fig. 8. A molecular model of a CNT in PS matrix, the CNT is pulled out half way from the matrix.

matrix may result in nano-mechanical interlocking, an effect similar to the clench of gears.

3. Mismatch in CTEs is a significant factor contributing to both non-bond interactions and mechanical interlocking, because compressive thermal residual stress may increases the true 'contact' area between CNT and the surrounding polymers.

From previous experimental studies and results of molecular modeling in this study, it has been suggested that the interfacial shear stress of CNT/polymer systems is at least an order of magnitude higher that micro fiber reinforced composites. It is believed that the high CNT-polymer interfacial shear stress from molecular simulation is attributed, to a large extent, to the intimate contact between CNT and the polymer matrix at the nanometer scale. CNTs offer a much smooth contact surface deprived of local cavities for polymer adsorption, as contrast to polymer-micro fiber interface which might be full of local irregularities that are prone for micro crack development under applied load.

4. Conclusions

We have studied local fracture morphologies of CNT/PS rod and CNT/epoxy film composites. Apparent strong interfacial adhesion between CNT and the matrices observed from electron microscopy is supported by results from molecular mechanics simulations and micromechanics calculations. In addition to inherent non-bond interactions, MWNT morphology-related mechanical interlocking at nanometer scale, thermal residual stresses, as well as relatively cavity free surface for polymer adsorption are also believed to be contributing factors.

Acknowledgements

The financial support from Nanyang Technological University under AcRF grant 34/99 is gratefully acknowledged. The authors would also like to thank Dr Ping Chen of National University of Singapore for her help in CNT synthesis.

References

[1] Ijima S. Nature 1991;354:56.
[2] Dresselhaus MS, Dresselhaus G, Avouris PH, editors. Carbon nanotubes synthesis, structure, properties, and applications. Springer: Berlin; 2001.
[3] Li F, Cheng HM, Bai S, Su G, Dresselhaus MS. Appl Phys Lett 2000; 77(20):3161–4.
[4] Pan ZW, Xie SS, Lu L, Chang BH, Sun LF, Zhou WY, Wang G, Zhang DL. Appl Phys Lett 1999;74(21):3152–4154.
[5] Yu MF, Files BS, Arepalli S, Ruoff RS. Phys Rev Lett 2000;84(24): 5552–5.
[6] Yu MF, Lourie O, Dyer MJ, Moloni K, Kelly TF, Ruoff RS. Science 2000;287(5453):637–40.
[7] Bower C, Rosen R, Jin L, Han J, Zhou O. Appl Phys Lett 1999;74(22): 3317–9.
[8] Chang BH, Liu ZQ, Sun LF, Tang DS, Zhou WY, Wang G, Qian LX, Xie SS, Fen JH, Wan MX. J Low Temp Phys 2000;119(1/2):41–8.
[9] Jia Z, Wang Z, Xu C, Liang J, Wei B, Wu D, Zhu S. Mater Sci Engng A 1999;271:395–400.
[10] Wagner HD, Lourie O, Feldman Y, Tenne R. Appl Phys Lett 1998; 72(2):188–90.
[11] Lourie O, Wagner HD. Appl Phys Lett 1998;73(24):3527–9.
[12] Qian D, Dickey EC, Andrew R, Rantell T. Appl Phys Lett 2000; 76(20):2868–70.
[13] Xu XJ, Thwe MM, Shearwood C, Liao K. Appl Phys Lett 2002; 81(15):2833–5.
[14] Wagner HD. Chem Phys Lett 2002;361:57–61.
[15] Liao K, Li S. Appl Phy Lett 2001;79(25):4225–7.
[16] Lordi V, Yao N. J Mater Res 2000;15(12):2770–9.
[17] Cooper CA, Cohen SR, Barber AH, Wagner HD. Appl Phys Lett 2002;81(20):3873–5.
[18] Schadler LS, Giannaris SC, Ajayan PM. Appl Phys Lett 1998;73(26): 3842–4.
[19] Ajayan PM, Schadler LS, Giannaris SC, Rubio A. Adv Mater 2000; 12(10):750–3.
[20] Wan KT, Liao K. Thin Solid Films 1999;352:167–72.
[21] Jin L, Bower C, Zhou O. Appl Phys Lett 1998;73(9):1197–9.
[22] Li Q, Liao K. Unpublished data.
[23] HyperChem® Computational chemistry, Canada: Hypercube, Inc., 1996.
[24] Liao K, Tan YM. Compos Part B: Engng 2001;32:365–70.
[25] Lu JP. Phys Rev Lett 1997;79(7):1297–300.
[26] Kelly BT. Physics of graphite. London: Applied Science Publishers; 1981.
[27] Shackelford JF, Alexander W, editors. Materials science and engineering handbook. Boca Raton: CRC Press; 1990.
[28] Ren Y, Liao K. Submitted.
[29] Lau KT. Chem Phys Lett 2003;370:399–405.